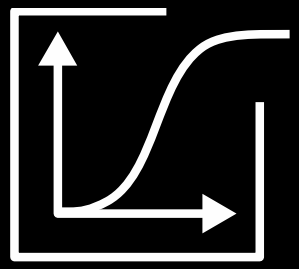

SOURCE DATA

Thomas Lemberger

Chief Editor, Molecular Systems Biology
Deputy Head, Scientific Publications, EMBO

EMBO
excellence in life sciences

EMBOpress

THE EMBO JOURNAL

EMBO reports

molecular systems biology
OPEN ACCESS

EMBO Molecular Medicine
OPEN ACCESS

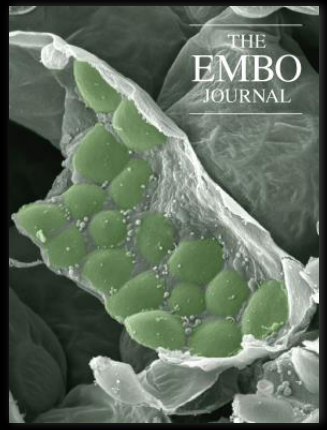

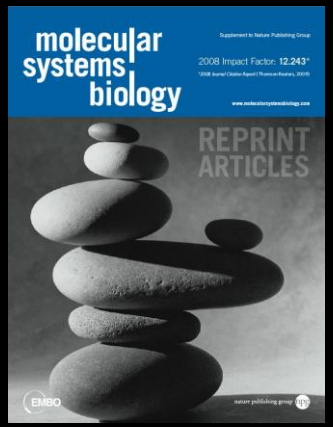

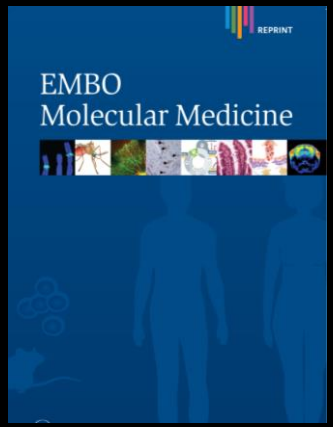

HighWire
Stanford University

EMBO
excellence in life sciences

WILEY

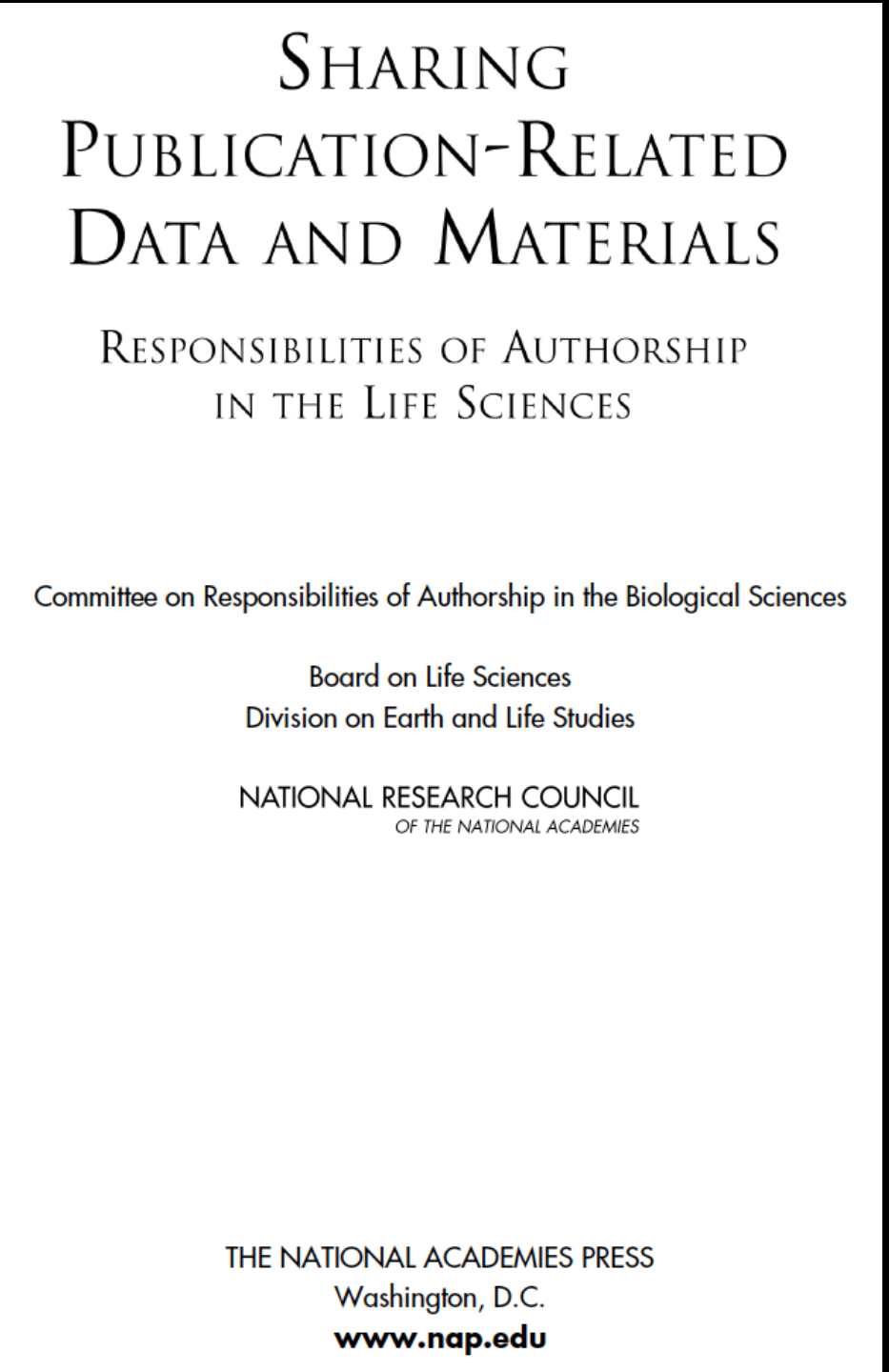

Scientific publishing

The publication of scientific information is intended to move science forward. More specifically, the act of publishing is a *quid pro quo* in which authors receive credit and acknowledgment in exchange for disclosure of their scientific findings.

move science forward

credit

disclose findings

data

open data

data integrity

Big Data

Structured data

structures

sequences

functional genomics

proteomics

metabolomics

genotype phenotype

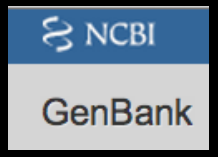

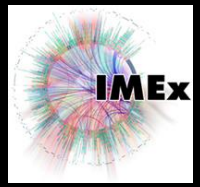

‘Publishing’ papers

‘Depositing’ datasets

"The two vital components of the scientific endeavor – the idea and the evidence – are too frequently separated"

Journals publish data!

Molecular Systems Biology 8; Article number 621 ; doi:10.1038/msb.2012.54
Citation: Molecular Systems Biology 8:621

1744-4292/12
www.molecularsystembiology.com

molecular systems biology

Competition between species can stabilize public-goods cooperation within a species

Hasan Celiker[1] and Jeff Gore[2,*]

[1] Department of Electrical Engineering and Computer Science, Massachusetts Institute of Technology, Cambridge, MA, USA and [2] Department of Physics, Massachusetts Institute of Technology, Cambridge, MA, USA
* Corresponding author. Department of Physics, Massachusetts Institute of Technology, 77 Massachusetts Avenue, 13-2008, Cambridge, MA 02139, USA. Tel.: +1 617 715 4251; Fax: +1 617 258 6883; E-mail: gore@mit.edu

Received 5.6.12; accepted 26.9.12

Competition between species is a major ecological force that can drive evolution. Here, we test the effect of this force on the evolution of cooperation within a species. We use sucrose metabolism of budding yeast, *Saccharomyces cerevisiae*, as a model cooperative system that is subject to social parasitism by cheater strategies. We find that when cocultured with a bacterial competitor, *Escherichia coli*, the frequency of cooperator phenotypes in yeast populations increases dramatically as compared with isolated yeast populations. Bacterial competition stabilizes cooperation within yeast by limiting the yeast population density and also by depleting the public goods produced by cooperating yeast cells. Both of these changes induced by bacterial competition increase the cooperator frequency because cooperator yeast cells have a small preferential access to the public goods they produce; this preferential access becomes more important when the public good is scarce. Our results indicate that a thorough understanding of species interactions is crucial for explaining the maintenance and evolution of cooperation in nature.

Molecular Systems Biology 8: 621; published online 13 November 2012; doi:10.1038/msb.2012.54
Subject Categories: simulation and data analysis; microbiology & pathogens
Keywords: cooperation; ecology; evolution; interspecies competition

Introduction

Cooperation is a widespread phenomenon in nature. However, costly cooperative strategies are vulnerable to exploitation by cheats that do not cooperate but freeload on the benefits produced by the cooperating individuals (Axelrod and Hamilton, 1981; Nowak, 2006). Therefore, the persistence of cooperation in nature has been a puzzling question for evolutionary biologists and there has been much theoretical and experimental research trying to elucidate the mechanisms underlying this phenomenon (Frank, 1998; West, 2007; West *et al*, 2007; Nowak *et al*, 2010). Microbial studies have suggested that cooperation can be maintained in nature by mechanisms such as reciprocity (Queller *et al*, 2003; Smukalla *et al*, 2009), spatial or temporal heterogeneity (Rainey and Rainey, 2003; MacLean and Gudelj, 2006; Diggle *et al*, 2007), and multilevel selection (Chuang *et al*, 2009). Recently, it has become increasingly clear that in addition to population dynamics, external ecological factors can also have significant roles in affecting the evolution of cooperation (Brockhurst *et al*, 2007, 2010).

One such important ecological factor is interspecies interactions (Little *et al*, 2008). However, almost all laboratory experiments aimed at understanding cooperation have relied on studying a single species in isolation. In contrast, species in the wild live and evolve within complex communities where they interact with other species (Thompson, 1999). Interspecific competition—that is competition between species—has been shown to have a key role in shaping species distributions (Connell, 1961; Schoener, 1983) and evolution of character displacement (Schluter, 1994; Grant and Grant, 2006). Nevertheless, little effort has focused on establishing a link between this ecological pressure and the evolution of cooperation within a species (Harrison *et al*, 2008; Hibbing *et al*, 2010; Korb and Foster, 2010; Mitri *et al*, 2011). As one of the few studies that tried to answer this question, Harrison *et al* found that interspecific competition with *Staphylococcus aureus* can select for cheats within *Pseudomonas aeruginosa* for the production of an iron-scavenging siderophore molecule. The authors speculated that this result was probably owing to increased competition for iron (Harrison *et al*, 2008). In another study, computer simulations of biofilms showed that in spatially structured environments, when competition for essential nutrients is strong, the addition of more species can inhibit cooperation within a focal species because the added species can outcompete the cooperating cells (Mitri *et al*, 2011). On the other hand, when nutrients were abundant, their model predicted that the public-good-producing cells would be surrounded by other species and insulated from cheater cells of the same species, thus cooperators would be favored. In our paper, we aimed to systematically quantify the effect of interspecific competition on the evolution of cooperation using an experimental microbial system, yeast sucrose metabolism. We found that the presence of a bacterial

competitor could dramatically increase the cooperator frequency.

Wild-type yeast cells break down extracellular sucrose cooperatively by paying a metabolic cost (Supplementary Figure S1) to synthesize the enzyme invertase (Greig and Travisano, 2004; Gore *et al*, 2009). Invertase is secreted into the periplasmic space between the plasma membrane and the cell wall where it hydrolyzes sucrose to the sugars glucose and fructose. In a well-mixed environment, most of the sugars produced in this manner diffuse away to be consumed by other cells in the population, making the sugars a shared public good. Under these conditions, an invertase-knockout strain can act as a cheater that takes advantage of and invades a cooperating population. However, cooperator cells capture ~1% of the sugar they produce owing to a local glucose gradient (Gore *et al*, 2009; Dai *et al*, 2012). This preferential access to the public good provides cooperators an advantage when present at low frequency, as in this case there is little glucose for the cheaters to consume (experiments here are done in media with 4% sucrose and 0.005% glucose). The cooperator and cheater strategies are therefore mutually invasible, leading to steady-state coexistence between the two strategies in well-mixed batch culture (Gore *et al*, 2009).

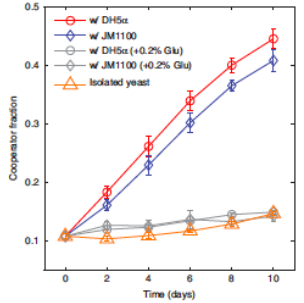

Figure 1 When cocultured with bacteria in sucrose media, cooperator cell fraction increases within yeast populations. Both with *E. coli* strains DH5α or JM1100—a mutant strain that grows poorly on glucose and fructose—a significant increase in cooperator fraction was observed compared with a pure yeast culture (isolated yeast) over 10 days of growth. Addition of excess glucose (+0.2%) to these cultures eliminated this increase in cooperator fraction, indicating that selection for cooperators is linked to sucrose metabolism. In this experiment, culture media contained 4 mM buffer (PIPES). Total final yeast and bacterial densities did not change significantly over the course of five cycles of growth (Supplementary Figure S9). Error bars, ± s.e.m. ($n = 3$). Source data is available for this figure in the Supplementary Information.

Results

Effect of interspecific competition on the evolution of cooperation within yeast

First, we confirmed that there is coexistence between cooperator and cheater strategies in pure yeast cultures. Starting with an initial cooperator fraction of 10%, we observed little change in cooperator frequency after 10 days of coculture (Figure 1). In these experiments, every 48 h we performed serial dilutions into fresh sucrose media and measured the fraction of cooperator cells within the yeast population using flow cytometry (Materials and methods and Supplementary Figure S2).

To test whether interspecific competition can influence cooperation within the yeast population, we performed the same experiment, but this time cocultured the cooperator and cheater yeast along with a bacterial competitor, *E. coli* (DH5α). This strain of *E. coli* cannot utilize sucrose (Reid and Abratt, 2005) but could grow on arabinose (another carbon source present in the media), on the other hand arabinose could not be utilized by our yeast strains (Supplementary Figure S3). We found that the presence of bacteria led to a large and rapid increase in the cooperator fraction in the yeast population over the 10 days of growth. Whereas the cooperator fraction in the pure yeast cultures was only ~14% at the end of the experiment, in cultures with the bacterial competitor the cooperator fraction increased to ~45% (Figure 1). We also confirmed that this increase in cooperator frequency is not due to a hidden fitness difference between the two yeast strains uncovered by the presence of bacteria. Addition of excess glucose (0.2%) completely eliminated any increase in cooperation in all of the tested conditions, even though bacteria were still present (Supplementary Figure S4). Therefore, the increase in cooperator fraction upon addition of the bacterial competitor is indeed related to sucrose metabolism.

A possible explanation for this increase in cooperator fraction within the yeast population is that bacteria behave as a 'superior' cheater strain by assimilating available free glucose, thus depriving cheater yeast cells of any sugar. In such a scenario, cooperator cells would do better than cheaters as they have at least some preferential access to the produced glucose. To test this, we competed yeast against a mutant strain of *E. coli* (JM1100) that has much reduced glucose and fructose uptake rates (Materials and methods) (Henderson *et al*, 1977). We found a somewhat smaller albeit still significant increase in the cooperator fraction within the yeast population under the same conditions (Figure 1). Bacterial competition for the public good may therefore be a contributing factor toward increasing cooperator frequency in the yeast population, but there is another mechanism at work as well. We will show later that the other mechanism by which bacterial competition is selecting for cooperator cells in yeast is by limiting the yeast population density.

Two-species growth dynamics

To gain insight into the dynamics of competition between the two species, we monitored the optical absorbance of batch cultures seeded with yeast and bacteria. We found that the overall growth follows reproducible successional stages (Figure 2A). Bacteria have a higher growth rate than yeast

Scientific publishing

- Dominant channel for the dissemination of peer-reviewed data.
- Journals function as a proxy for quality in research assessment

- The rate of publishing keeps increasing.
- Papers are human-readable but poorly machine-readable.

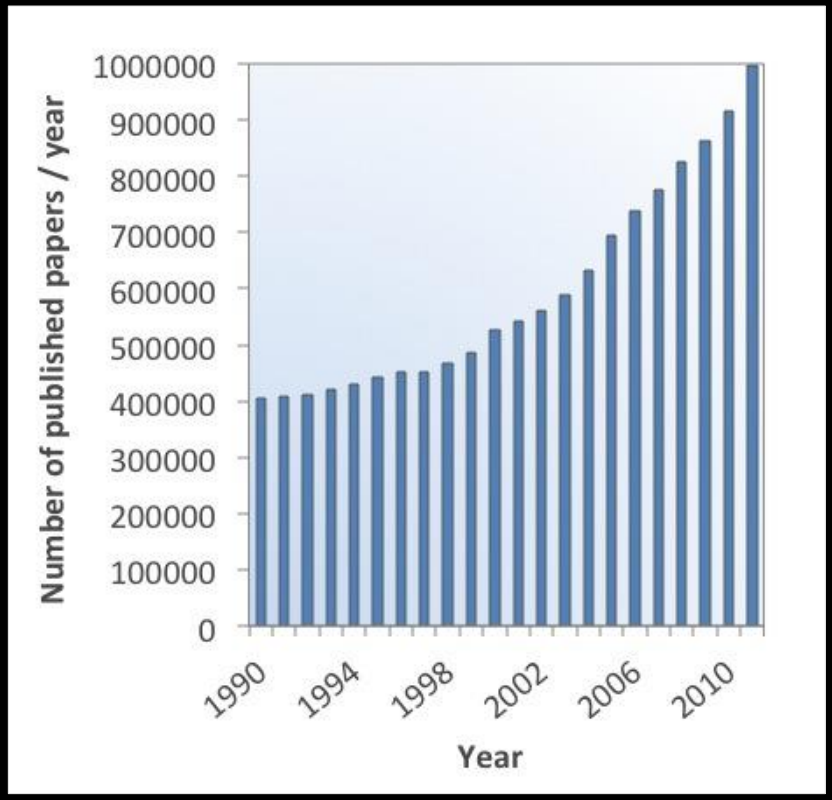


search

The Economist

OCTOBER 19TH–25TH 2013

Economist.com

Washington's lawyer surplus

How to do a nuclear deal with Iran

Investment tips from Nobel economists

Junk bonds are back

The meaning of Sachin Tendulkar

HOW SCIENCE GOES WRONG

99

Einsteinium

What is a paper?

Title

Abstract

Synopsis

Main paper

‘Expanded view’

Datasets & code

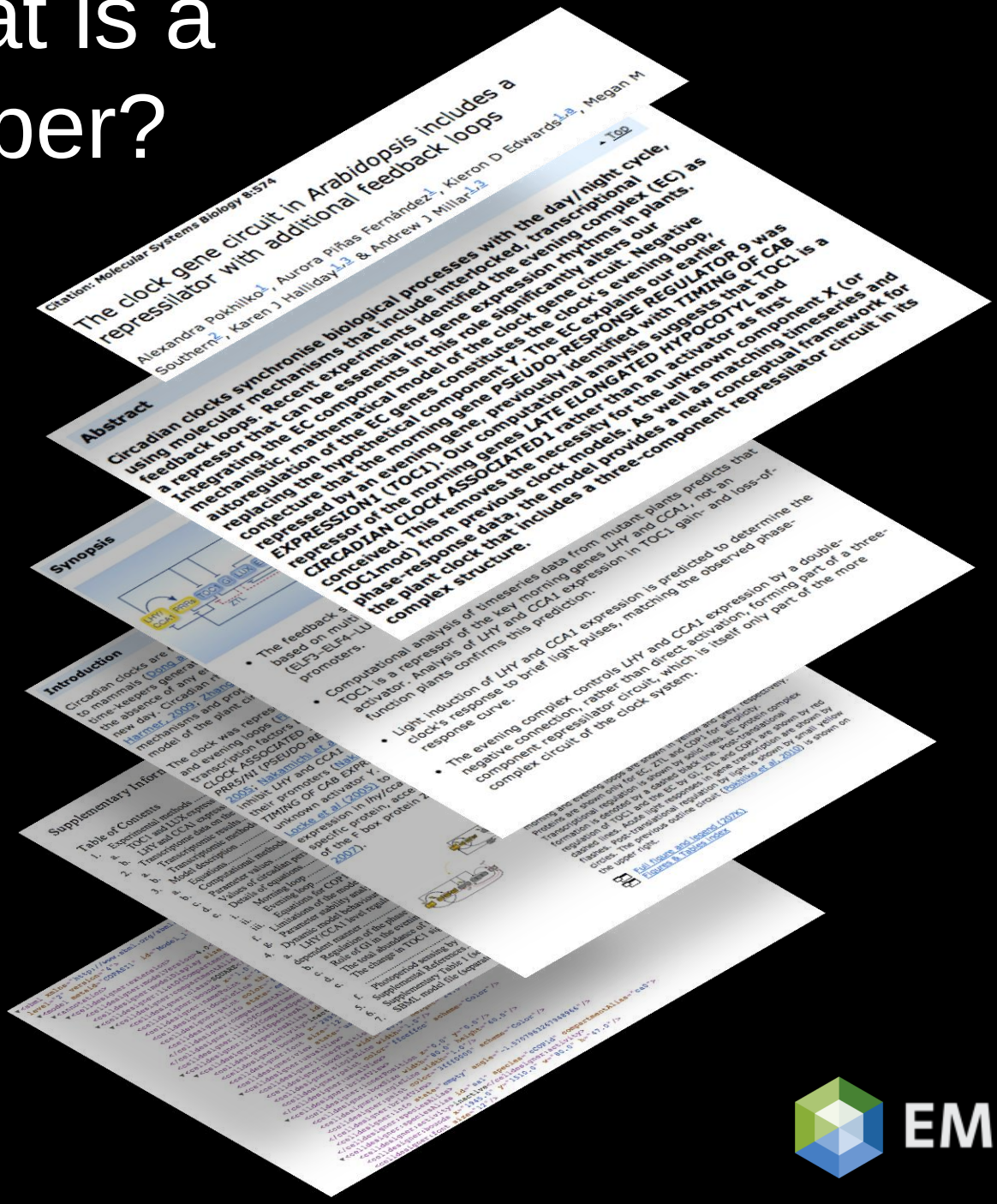

mTORC1 signaling is positively regulated by growth factors through the PI3K-AKT pathway (Growth Factor/Nutrient module in Figures 2 and 3). The binding of insulin to its cell surface receptor leads to the recruitment and phosphorylation of IRS-1, which promotes the recruitment and activation of PI3K at the cell surface membrane. Active PI3K converts phosphatidylinositol-4,5-phosphate to phosphatidylinositol-3,4,5-phosphate (PIP3), a process antagonized by the lipid phosphatase PTEN. When produced at the plasma membrane, PIP3 recruits both PDK1 and AKT, resulting in the phosphorylation and partial activation of AKT. Whereas PDK1 phosphorylates AKT at Thr308, additional phosphorylation at Ser473 by mTORC2 (see below) is necessary for optimal activation of AKT in vitro (Sarbassov et al, 2005). mTORC1 is thought to be activated in part by AKT through the tuberous sclerosis complex proteins, TSC1 and TSC2. The TSC1-TSC2 complex is a critical negative regulator of mTORC1 (Huang and Manning, 2008b). Because of its central role in regulating mTORC1, 34 species depicting extensive details about the TSC1-TSC2 complex (post-translation modifications, interactors, cellular locations) were represented in the comprehensive mTOR map. In response to growth factors, TSC2 is phosphorylated and functionally inactivated by AKT (Inoki et al, 2002; Manning et al, 2002). ERK1/2 and RSK1/2 were also shown to phosphorylate and inactivate TSC2 in response to growth factors (Roux et al, 2004; Ballif et al, 2005; Ma et al, 2005), suggesting that PI3K and Ras/MAPK pathways collaborate to inhibit TSC1-TSC2 function in response to growth factors. Whereas TSC2 functions as a GAP toward the small Ras-related GTPase Rheb, TSC1 is required to stabilize TSC2 and prevent its proteasomal degradation (Huang and Manning, 2008b). While the active GTP-bound form of Rheb was shown to directly interact with mTOR to stimulate its catalytic activity (Long et al, 2005), Rheb may also promote substrate recognition by mTORC1 (Sancak et al, 2007; Sato et al, 2009). Nutrients, such as amino acids, regulate mTORC1 signaling via different mechanisms. Amino acid availability regulates mTORC1 in a TSC2-independent but Rheb-dependent manner (Smith et al, 2005; Gulati and Thomas, 2007), but the exact mechanism remains poorly understood (Growth Factor/Nutrient module in Figures 2 and 3). Two complementary studies have provided compelling evidence that the Rag family of small GTPases is both necessary and sufficient to transmit a positive signal from amino acids to mTOR (Kim et al, 2008; Sancak et al, 2008). The current model proposes that amino acids induce the movement of mTORC1 to lysosomal membranes, where Rag proteins reside. More precisely, a complex encoded by the MAPKSP1, ROBLD3 and c11orf59 genes, interacts with the Rag GTPases, recruits them to lysosomes, and was shown to be essential for mTORC1 activation (Sancak et al, 2010). mTORC1 activity is sensitive to oxygen deprivation, and one pathway by which this occurs involves activation of the TSC1-TSC2 complex by REDD1, a hypoxia-inducible protein (Hypoxia module in Figures 2 and 3l; Brugarolas et al, 2004). Newly synthesized REDD1 was found to interact with 14-3-3 and relieve TSC2 from 14-3-3-dependent repression (DeYoung et al, 2008). mTORC1 also senses insufficient cellular energy levels through AMPK, a protein kinase activated in response to a low ATP/AMP ratio (Inoki et al, 2003) and by LKB1-mediated phosphorylation (Low Energy module in

mTORC1 signaling is positively regulated by growth factors through the PI3K-AKT pathway (Growth Factor/Nutrient module in Figures 2 and 3). The binding of **insulin** to its cell **surface receptor** leads to the recruitment and phosphorylation of **IRS-1**, which promotes the recruitment and activation of **PI3K** at the cell surface membrane. Active PI3K converts phosphatidylinositol-4,5-phosphate to phosphatidylinositol-3,4,5-phosphate (**PIP3**), a process antagonized by the lipid phosphatase **PTEN**. When produced at the plasma membrane, PIP3 recruits both **PDK1** and **AKT**, resulting in the phosphorylation and partial activation of AKT. Whereas PDK1 phosphorylates AKT at Thr308, additional phosphorylation at Ser473 by mTORC2 (see below) is necessary for optimal activation of AKT in vitro (Sarbassov et al, 2005). **mTORC1** is thought to be activated in part by AKT through the tuberous sclerosis complex proteins, TSC1 and TSC2. The **TSC1-TSC2 complex** is a critical negative regulator of mTORC1 (Huang and Manning, 2008b). Because of its central role in regulating mTORC1, 34 species depicting extensive details about the TSC1-TSC2 complex (post-translation modifications, interactors, cellular locations) were represented in the comprehensive mTOR map. In response to growth factors, TSC2 is phosphorylated and functionally inactivated by AKT (Inoki et al, 2002; Manning et al, 2002). **ERK1/2** and **RSK1/2** were also shown to phosphorylate and inactivate TSC2 in response to growth factors (Roux et al, 2004; Ballif et al, 2005; Ma et al, 2005), suggesting that PI3K and Ras/MAPK pathways collaborate to inhibit TSC1-TSC2 function in response to growth factors. Whereas TSC2 functions as a GAP toward the small Ras-related GTPase Rheb, TSC1 is required to stabilize TSC2 and prevent its proteasomal degradation (Huang and Manning, 2008b). While the active GTP-bound form of Rheb was shown to directly interact with mTOR to stimulate its catalytic activity (Long et al, 2005), Rheb may also promote substrate recognition by mTORC1 (Sancak et al, 2007; Sato et al, 2009). Nutrients, such as amino acids, regulate mTORC1 signaling via different mechanisms. Amino acid availability regulates mTORC1 in a TSC2-independent but Rheb-dependent manner (Smith et al, 2005; Gulati and Thomas, 2007), but the exact mechanism remains poorly understood (Growth Factor/Nutrient module in Figures 2 and 3). Two complementary studies have provided compelling evidence that the Rag family of small GTPases is both necessary and sufficient to transmit a positive signal from amino acids to mTOR (Kim et al, 2008; Sancak et al, 2008). The current model proposes that amino acids induce the movement of mTORC1 to lysosomal membranes, where Rag proteins reside. More precisely, a complex encoded by the MAPKSP1, ROBLD3 and c11orf59 genes, interacts with the Rag GTPases, recruits them to lysosomes, and was shown to be essential for mTORC1 activation (Sancak et al, 2010). mTORC1 activity is sensitive to oxygen deprivation, and one pathway by which this occurs involves activation of the TSC1-TSC2 complex by REDD1, a hypoxia-inducible protein (Hypoxia module in Figures 2 and 3l; Brugarolas et al, 2004). Newly synthesized REDD1 was found to interact with 14-3-3 and relieve TSC2 from 14-3-3-dependent repression (DeYoung et al, 2008). mTORC1 also senses insufficient cellular energy levels through AMPK, a protein kinase activated in response to a low ATP/AMP ratio (Inoki et al, 2003) and by LKB1-mediated phosphorylation (Low Energy module in

mTORC1 signaling is positively regulated by growth factors through the PI3K-AKT pathway (Growth Factor/Nutrient module in Figures 2 and 3). The binding of **insulin** to its cell **surface receptor** leads to the recruitment and phosphorylation of **IRS-1**, which promotes the recruitment and activation of **PI3K** at the cell surface membrane. Active PI3K converts phosphatidylinositol-4,5-phosphate to phosphatidylinositol-3,4,5-phosphate (**PIP3**), a process antagonized by the lipid phosphatase **PTEN**. When produced at the plasma membrane, PIP3 recruits both **PDK1** and **AKT**, resulting in the phosphorylation and partial activation of AKT. Whereas PDK1 phosphorylates AKT at Thr308, additional phosphorylation at Ser473 by mTORC2 (see below) is necessary for optimal activation of AKT in vitro (Sarbassov et al, 2005). **mTORC1** is thought to be activated in part by AKT through the tuberous sclerosis complex proteins, TSC1 and TSC2. The **TSC1-TSC2 complex** is a critical negative regulator of mTORC1 (Huang and Manning, 2008b). Because of its central role in regulating mTORC1, 34 species depicting extensive details about the TSC1-TSC2 complex (post-translation modifications, interactors, cellular locations) were represented in the comprehensive mTOR map. In response to growth factors, TSC2 is phosphorylated and functionally inactivated by AKT (Inoki et al, 2002; Manning et al, 2002). **ERK1/2** and **RSK1/2** were also shown to phosphorylate and inactivate TSC2 in response to growth factors (Roux et al, 2004; Ballif et al, 2005; Ma et al, 2005), suggesting that PI3K and Ras/MAPK pathways collaborate to inhibit TSC1-TSC2 function in response to growth factors. Whereas TSC2 functions as a GAP toward the small Ras-related GTPase Rheb, TSC1 is required to stabilize TSC2 and prevent its proteasomal degradation (Huang and Manning, 2008b). While the active GTP-bound form of Rheb was shown to directly interact with mTOR to stimulate its catalytic activity (Long et al, 2005), Rheb may also promote substrate recognition by mTORC1 (Sancak et al, 2007; Sato et al, 2009). Nutrients, such as amino acids, regulate mTORC1 signaling via different mechanisms. Amino acid availability regulates mTORC1 in a TSC2-independent but Rheb-dependent manner (Smith et al, 2005; Gulati and Thomas, 2007), but the exact mechanism remains poorly understood (Growth Factor/Nutrient module in Figures 2 and 3). Two complementary studies have provided compelling evidence that the Rag family of small GTPases is both necessary and sufficient to transmit a positive signal from amino acids to mTOR (Kim et al, 2008; Sancak et al, 2008). The current model proposes that amino acids induce the movement of mTORC1 to lysosomal membranes, where Rag proteins reside. More precisely, a complex encoded by the MAPKSP1, ROBLD3 and c11orf59 genes, interacts with the Rag GTPases, recruits them to lysosomes, and was shown to be essential for mTORC1 activation (Sancak et al, 2010). mTORC1 activity is sensitive to oxygen deprivation, and one pathway by which this occurs involves activation of the TSC1-TSC2 complex by REDD1, a hypoxia-inducible protein (Hypoxia module in Figures 2 and 3l; Brugarolas et al, 2004). Newly synthesized REDD1 was found to interact with 14-3-3 and relieve TSC2 from 14-3-3-dependent repression (DeYoung et al, 2008). mTORC1 also senses insufficient cellular energy levels through AMPK, a protein kinase activated in response to a low ATP/AMP ratio (Inoki et al, 2003) and by LKB1-mediated phosphorylation (Low Energy module in

What is a figure?

A scientific result converted into a collection of pixels…

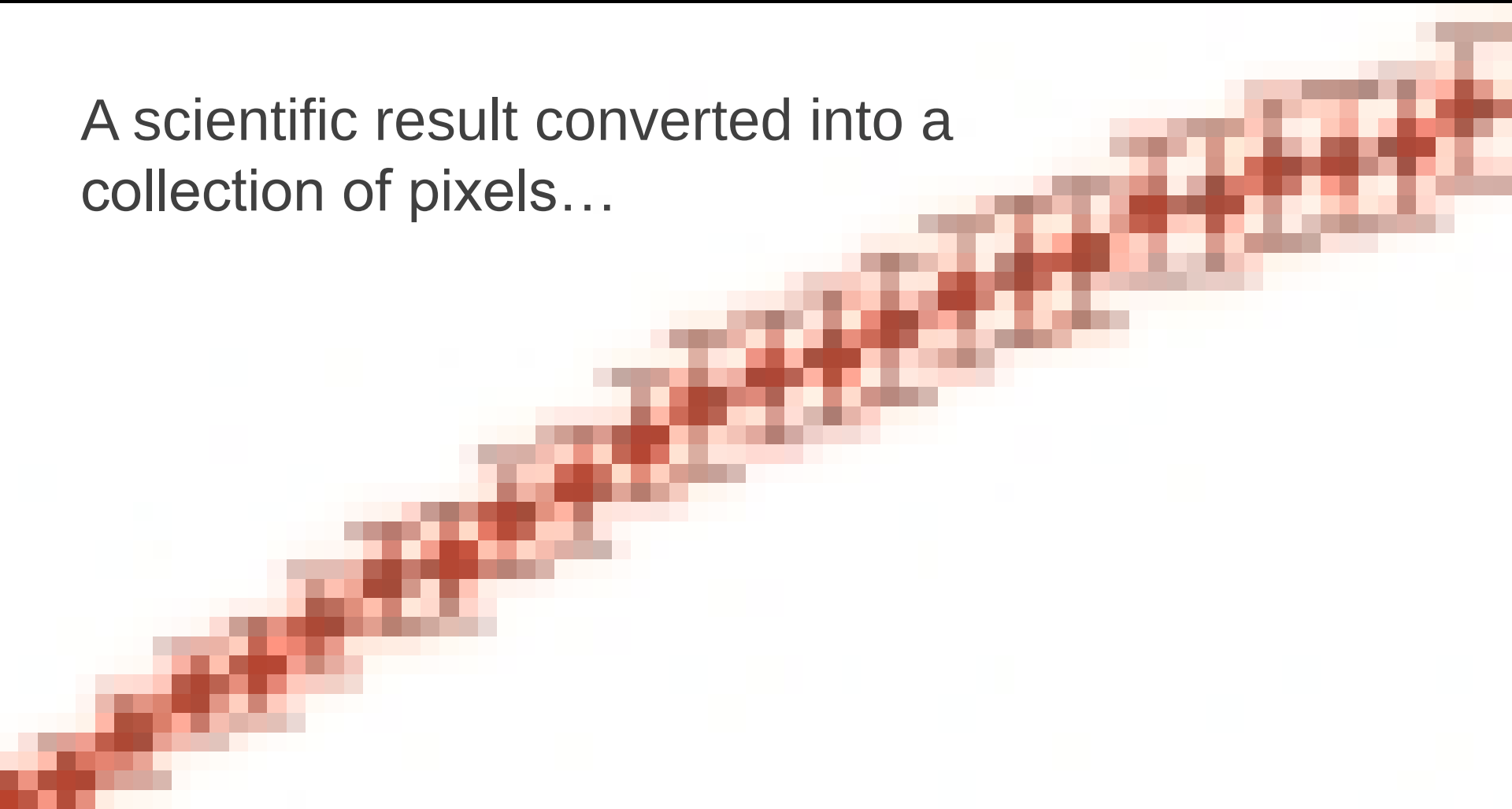

SourceData

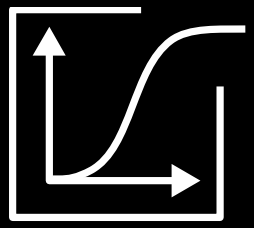

Tools to publish figures as structured digital objects that link the human-readable illustrations with machine-readable metadata and ‘source data’ in order to

- improve data transparency;
- make published data useable;
- enable data-oriented search.

EMBOpress

SourceData

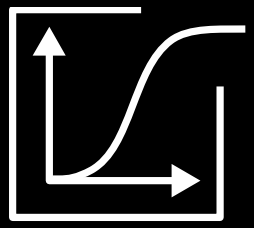

Data ⟷ Metadata ⟷ Search

- Figure source data files hosted by the journals
- Link to ‘unstructured data’ repositories

- Focus on the biological content
- Use standard identifiers and existing controlled vocabularies

- Data-oriented semantic search of the literature.
- Overcome some of the limitations of keyword-based search

EMBOpress

THE EMBO JOURNAL | EMBO reports | molecular systems biology | EMBO Molecular Medicine

Figure 1

Systematic analysis of PDGF-stimulated Erk phosphorylation kinetics. (**A**) Immunoblots, representative of five or six independent experiments, used to quantify relative amounts of phosphorylated Erk (p-Erk1/2) and total Erk (t-Erk1). NIH 3T3 fibroblasts were modulated by retroviral induction of dominant-negative (S17N) or constitutively active (G12V) H-Ras expression or incubation with inhibitors of PI3K (100 μM LY294002) or MEK (50 μM PD098059). The respective controls are empty pBM-puro vector or 0.2% DMSO. Lysates were prepared from cells that were unstimulated or stimulated with PDGF-BB for 5, 15, 30, 60, or 120 min. (**B–E**) Quantification of Erk phosphorylation, normalized as described under Materials and methods, comparing either S17N Ras expression (B; n=6), PI3K inhibition (C; n=5), G12V Ras expression (D; n=6), or MEK inhibition (E; n=5) with their respective controls. Values are reported as mean±s.e.m., and comparisons to control in (B, C) are by Student's t-test: $^{*}P<0.05$; $^{**}P<0.01$. Source data is available for this figure at www.nature.com/msb.

- Full figure and legend (660K)
- Source data for figure 1BD (6K)
- Source data for figure 1CE (5K)
- Figures & Tables Index

SOURCE DATA

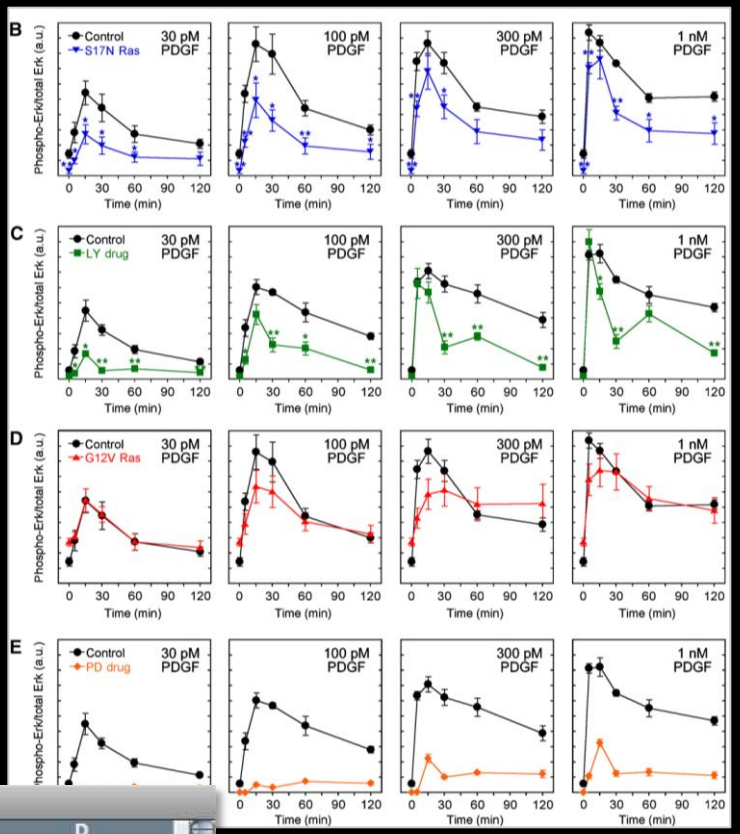

Fig1b&d_raw.txt

	A	B	C	D
1	Fig1b&d-Column1	Fig1b&d-Column2A	Fig1b&d-Column2B	Fig1b&d-Column2C
2	Time (min)	p-Erk/t-Erk, 30 pM PDGF, control vector, Expt. 1	p-Erk/t-Erk, 30 pM PDGF, control vector, Expt. 2	p-Erk/t-Erk, 30 pM PDGF, control vector, Expt. 3
3	0	0.194672394	0.201524091	0.339116171
4	5	0.395173883	0.389974466	0.555355249
5	15	0.690917146	1.236910363	1.632582883
6	30	0.394324884	0.72081196	1.488299981
7	60	0.38782972	0.38107614	0.428561181
8	120	0.384442827	0.216360469	0.458929493
9				
10				

Fig1b&d_raw.txt
Ready

EMBOpress

THE EMBO JOURNAL | EMBO reports | molecular systems biology | EMBO Molecular Medicine

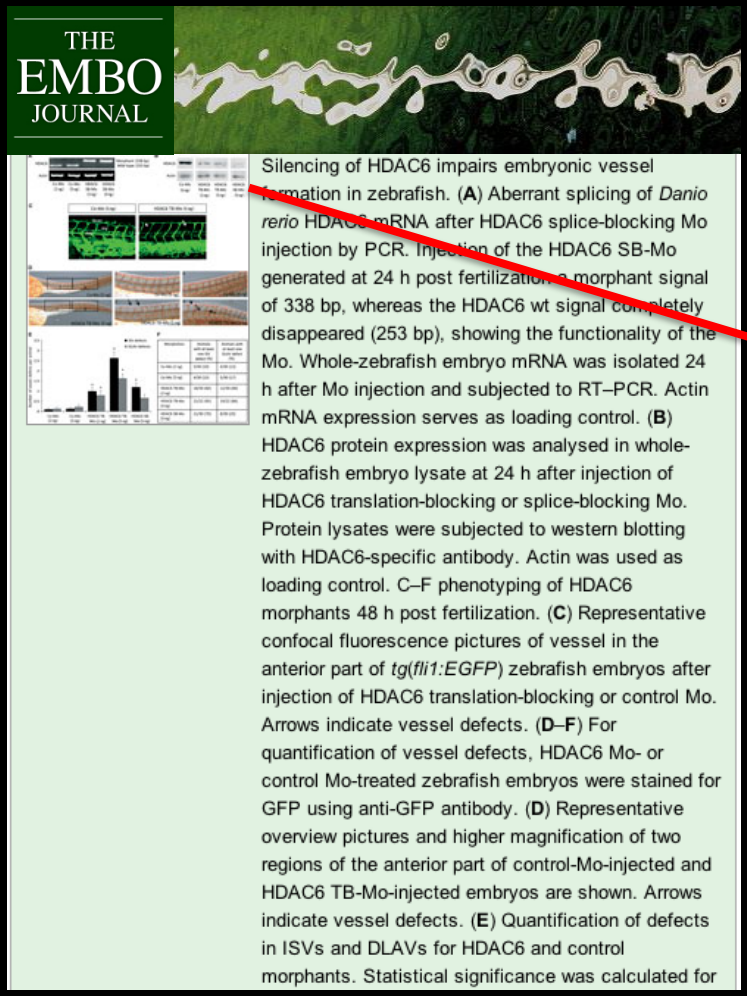

Silencing of HDAC6 impairs embryonic vessel formation in zebrafish. (**A**) Aberrant splicing of *Danio rerio* HDAC6 mRNA after HDAC6 splice-blocking Mo injection by PCR. Injection of the HDAC6 SB-Mo generated at 24 h post fertilization a morphant signal of 338 bp, whereas the HDAC6 wt signal completely disappeared (253 bp), showing the functionality of the Mo. Whole-zebrafish embryo mRNA was isolated 24 h after Mo injection and subjected to RT–PCR. Actin mRNA expression serves as loading control. (**B**) HDAC6 protein expression was analysed in whole-zebrafish embryo lysate at 24 h after injection of HDAC6 translation-blocking or splice-blocking Mo. Protein lysates were subjected to western blotting with HDAC6-specific antibody. Actin was used as loading control. C–F phenotyping of HDAC6 morphants 48 h post fertilization. (**C**) Representative confocal fluorescence pictures of vessel in the anterior part of *tg(fli1:EGFP)* zebrafish embryos after injection of HDAC6 translation-blocking or control Mo. Arrows indicate vessel defects. (**D–F**) For quantification of vessel defects, HDAC6 Mo- or control Mo-treated zebrafish embryos were stained for GFP using anti-GFP antibody. (**D**) Representative overview pictures and higher magnification of two regions of the anterior part of control-Mo-injected and HDAC6 TB-Mo-injected embryos are shown. Arrows indicate vessel defects. (**E**) Quantification of defects in ISVs and DLAVs for HDAC6 and control morphants. Statistical significance was calculated for

SOURCE DATA

Figure 4A

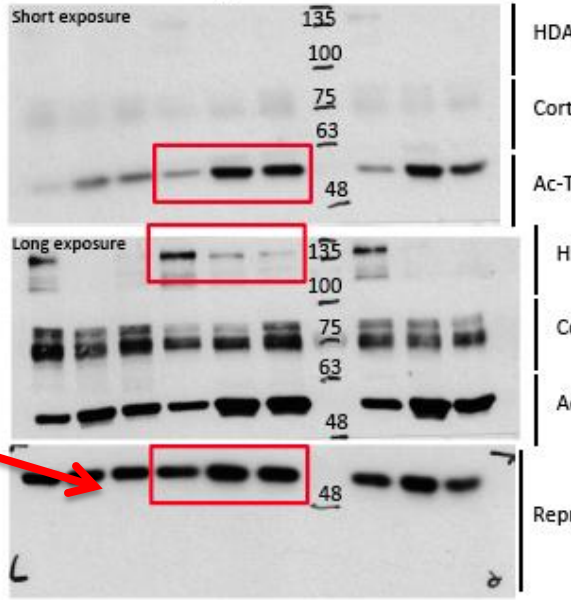

Figure 4G

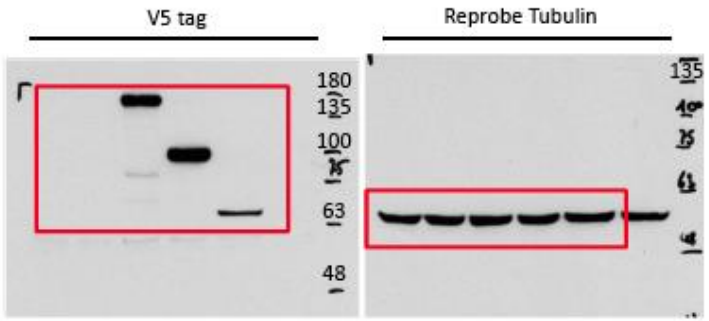

THE EMBO JOURNAL | EMBO reports | molecular systems biology | EMBO Molecular Medicine

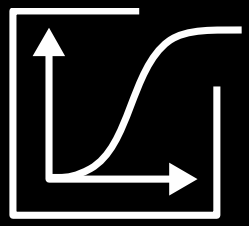

SOURCE DATA

- Data archival service
- Data ‘transparency’
- Data reuse
- Data-oriented search

Figure 1

Systematic analysis of PDGF-stimulated Erk phosphorylation kinetics. (**A**) Immunoblots, representative of five or six independent experiments, used to quantify relative amounts of phosphorylated Erk (p-Erk1/2) and total Erk (t-Erk1). NIH 3T3 fibroblasts were modulated by retroviral induction of dominant-negative (S17N) or constitutively active (G12V) H-Ras expression or incubation with inhibitors of PI3K (100 μM LY294002) or MEK (50 μM PD098059). The respective controls are empty pBM-puro vector or 0.2% DMSO. Lysates were prepared from cells that were unstimulated or stimulated with PDGF-BB for 5, 15, 30, 60, or 120 min. (**B–E**) Quantification of Erk phosphorylation, normalized as described under Materials and methods, comparing either S17N Ras expression (B; n=6), PI3K inhibition (C; n=5), G12V Ras expression (D; n=6), or MEK inhibition (E; n=5) with their respective controls. Values are reported as mean±s.e.m., and comparisons to control in (B, C) are by Student's t-test: $^{*}P<0.05$; $^{**}P<0.01$. Source data is available for this figure at www.nature.com/msb.

Full figure and legend (660K)
Source data for figure 1BD (6K)
Source data for figure 1CE (5K)
Figures & Tables index

Fig1 raw.txt

	A	B	C	D
1	Fig1b&d-Column1	Fig1b&d-Column2	Fig1b&d-Column2B	Fig1b&d-Column2C
2	Time (min)	p-Erk/t-Erk, 30 pM PDGF, control vector, Expt. 1	p-Erk/t-Erk, 30 pM PDGF, control vector, Expt. 2	p-Erk/t-Erk, 30 pM PDGF, control vector, Expt. 3
3	0	0.194672394	0.201524091	0.339116171
4	5	0.395173883	0.389974466	0.555355249
5	15	0.690917146	1.236910363	1.632582883
6	30	0.394324884	0.72081196	1.488299981
7	60	0.38782972	0.38107614	0.428561181
8	120	0.384442827	0.216360469	0.458929493
9				
10				

Fig1b&d_raw.txt
Ready

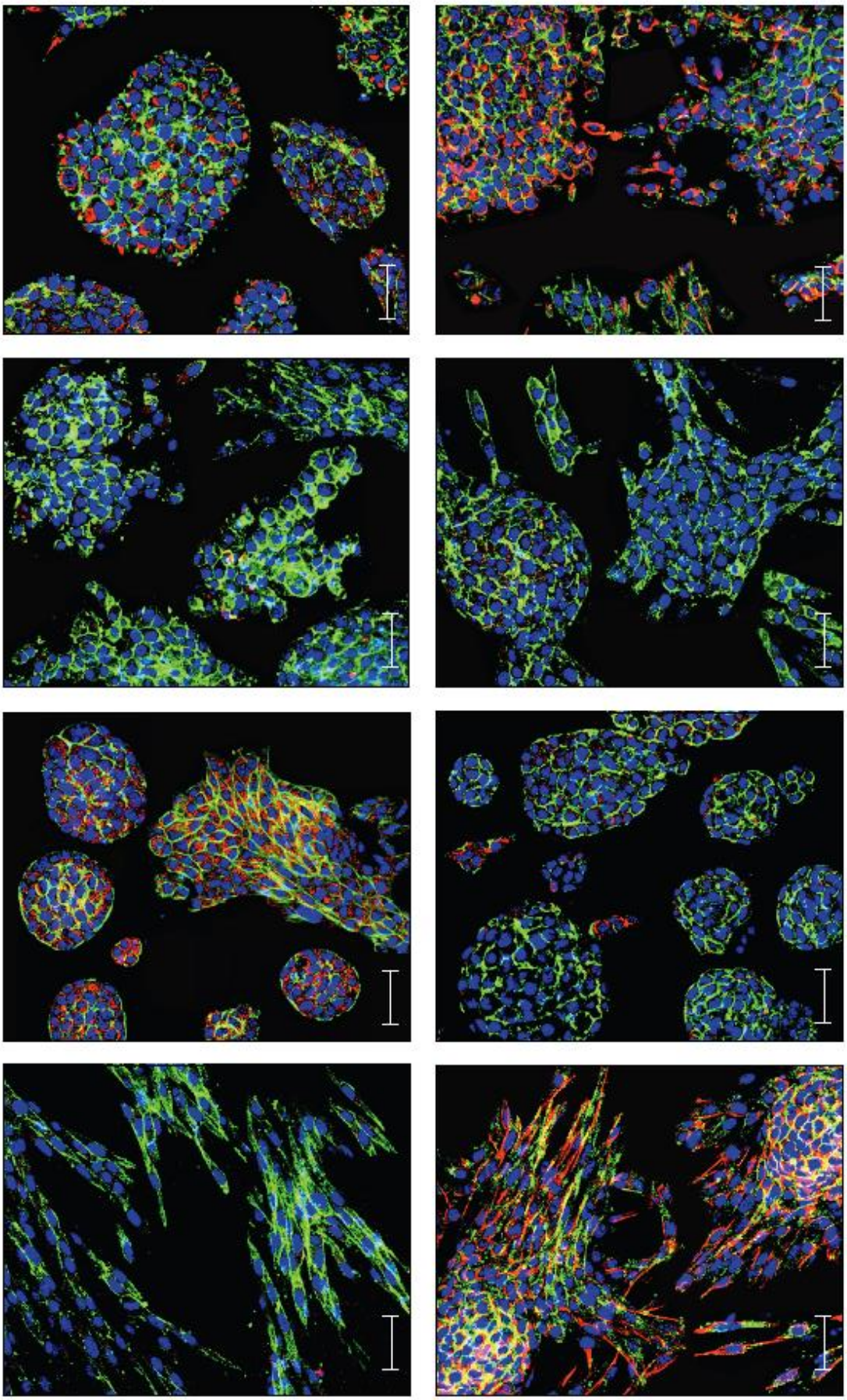
E-cadherin/ actin/ DNA
Vimentin/ actin/ DNA

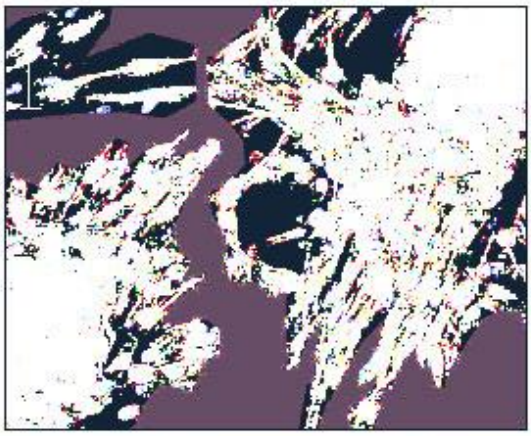
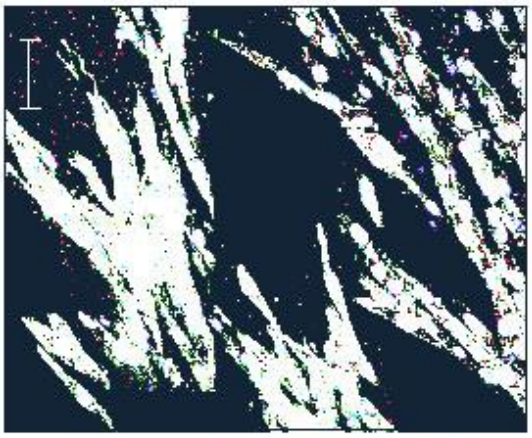
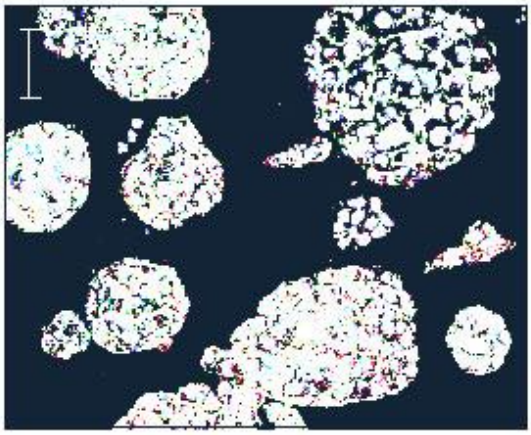
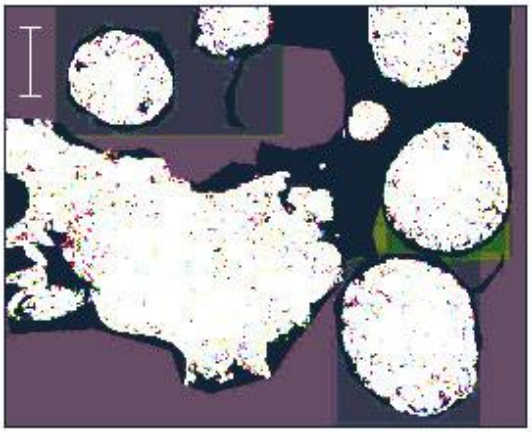
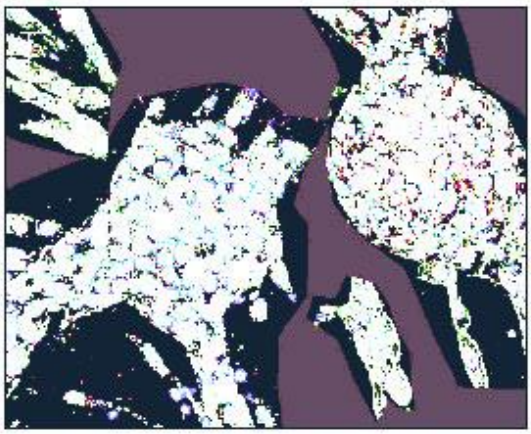
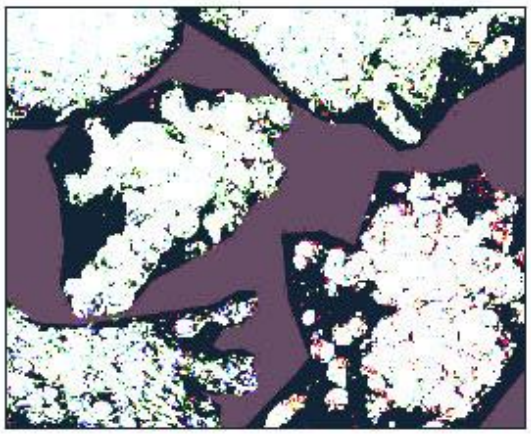
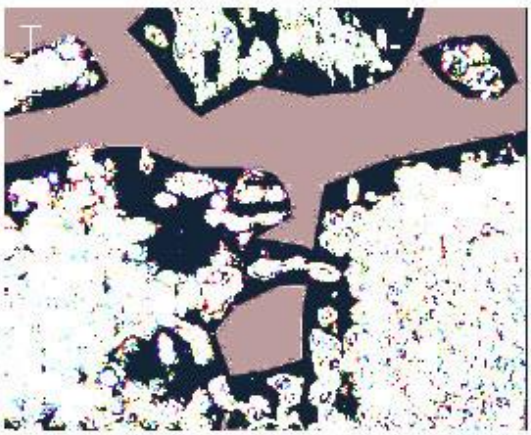
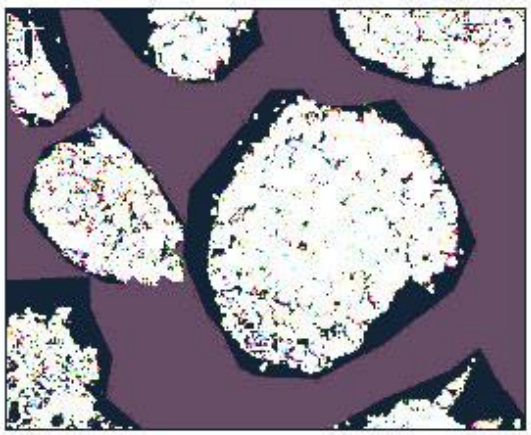

Title

Abstract

Synopsis

Main paper

Expert view

Actionable data

Molecular Systems Biology **6** Article number: 370 doi:10.1038/msb.2010.25
Published online: 8 June 2010
Citation: ***Molecular Systems Biology* 6:370**

molecular systems biology

Clustering phenotype populations by genome-wide RNAi and multiparametric imaging

Florian Fuchs[1,a], Gregoire Pau[2,3,a], Dominique Kranz[1], Oleg Sklyar[2], Christoph Budjan[1], Sandra Steinbrink[1], Thomas Horn[1], Angelika Pedal[1], Wolfgang Huber[2,3] & Michael Boutros[1]

SourceData

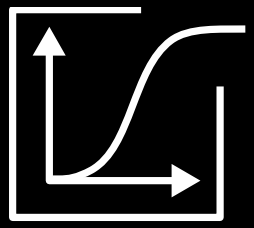

Data ⟷ Metadata ⟷ Search

- Figure source data files hosted by the journals
- Link to ‘unstructured data’ repositories

- Focus on the biological content
- Use standard identifiers and existing controlled vocabularies

- Data-oriented semantic search of the literature.
- Overcome some of the limitations of keyword-based search

EMBOpress

Structured metadata: ‘perturbation-observation-assay’

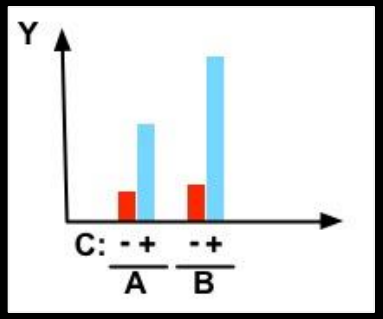

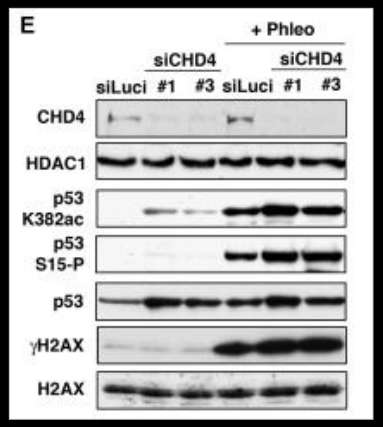

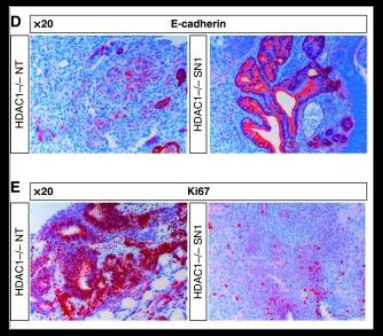

(Level 0: metadata associated to individual panels.)

Level 1: ‘object-oriented’ representation of experimental variables as a list of chemical and biological components.

Level 2: represent the causality of the experimental design: “Measurement of Y as a function of A, B, C, using assay P in biological system S.”

Level 3: machine-readable representation with standard identifiers.

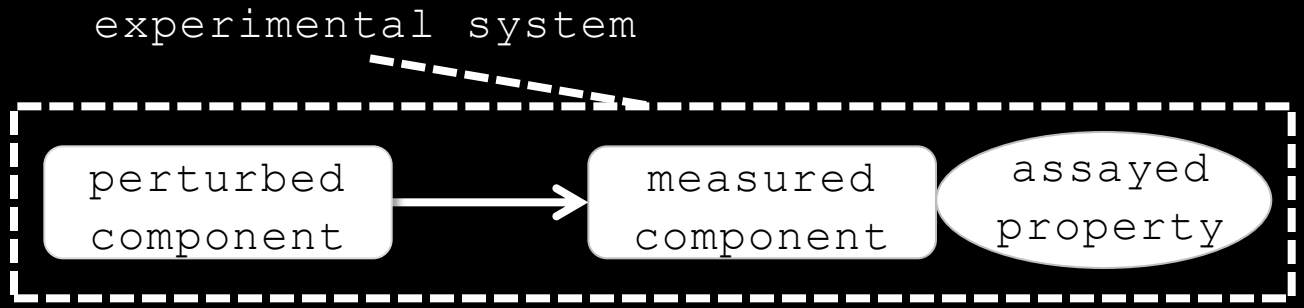

‘Data copy editors’

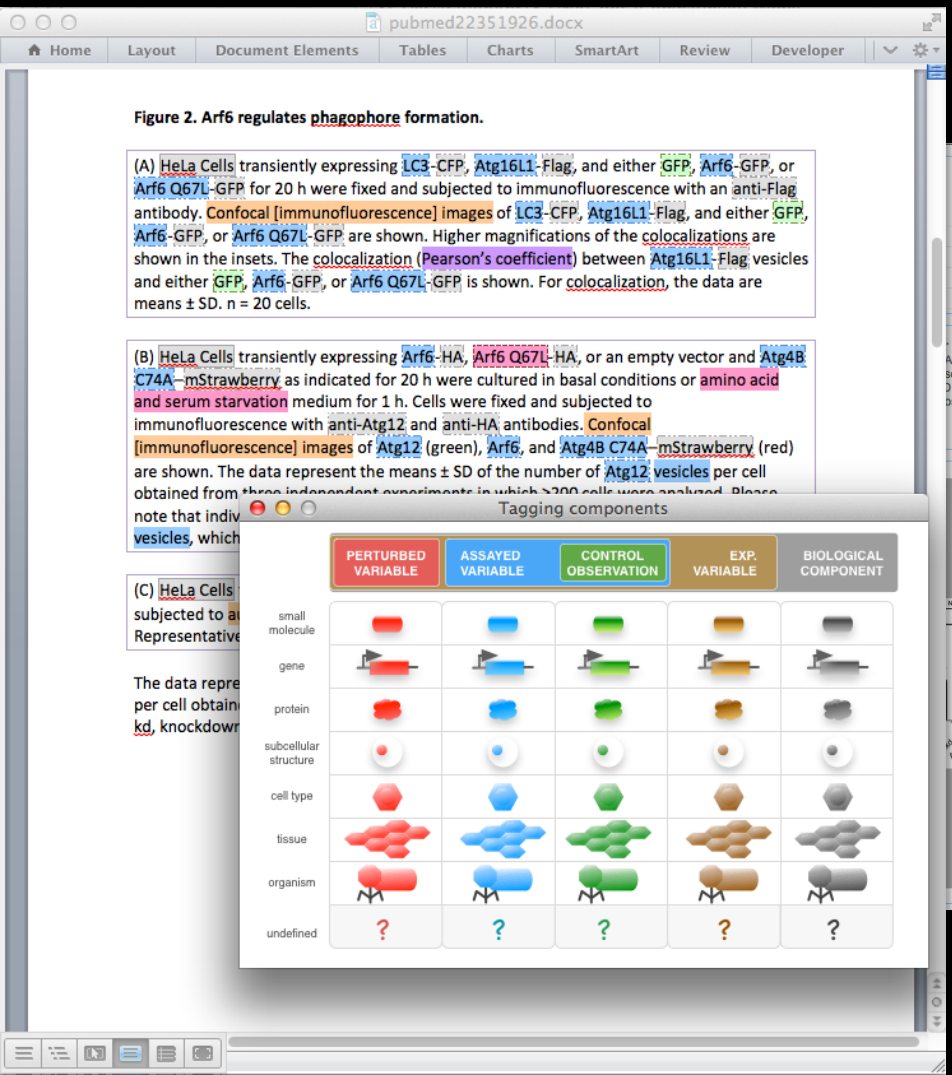

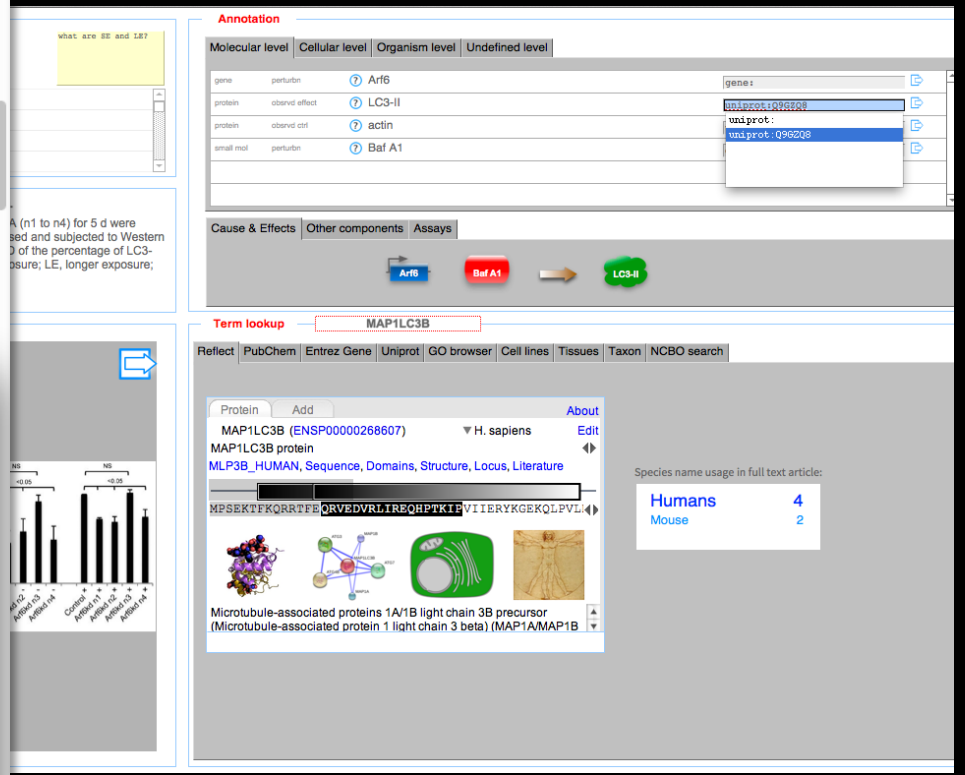

EMBOpress

Data workflow

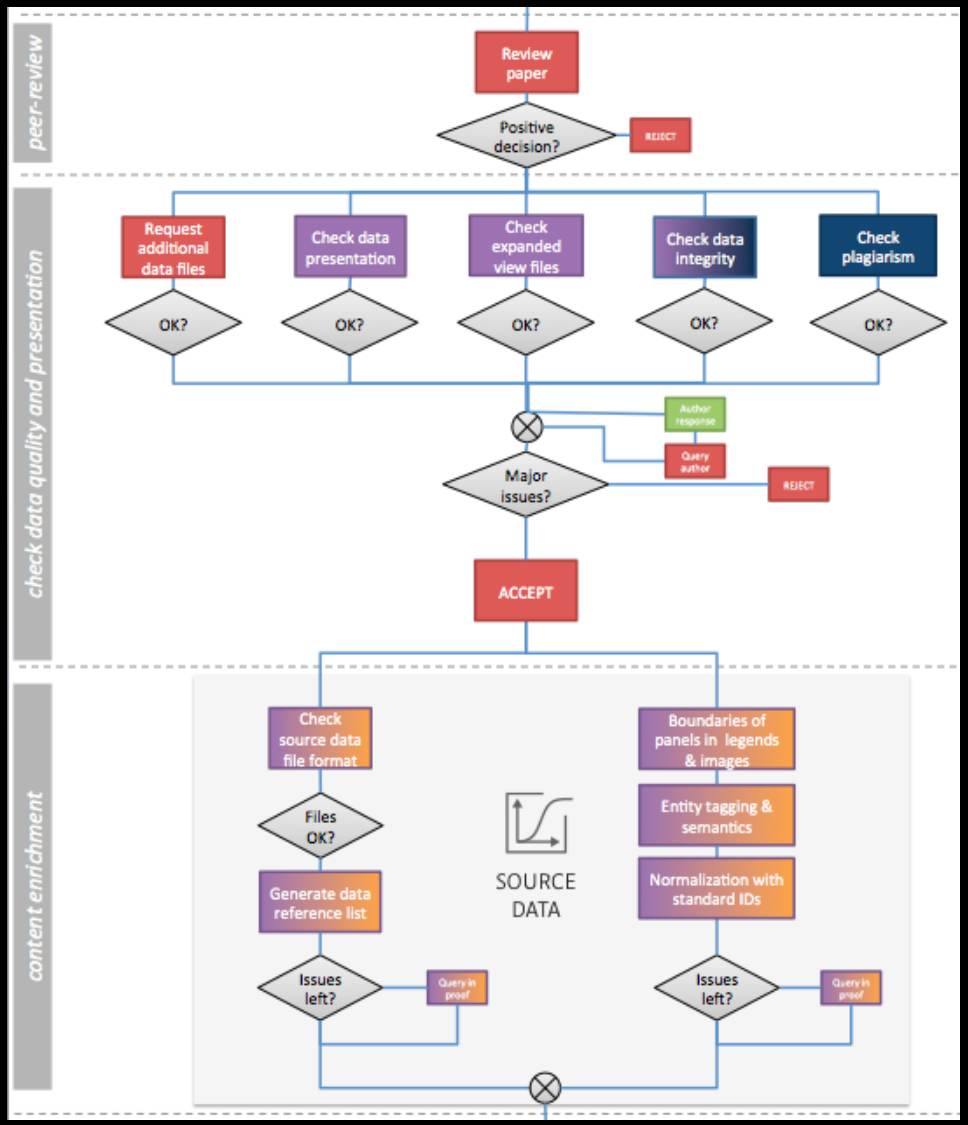

EMBOpress

SourceData

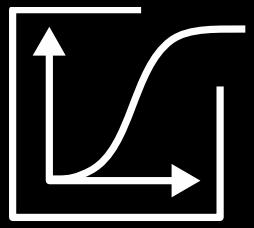

Data ⟷ Metadata ⟷ Search

- Figure source data files hosted by the journals
- Link to ‘unstructured data’ repositories

- Focus on the biological content
- Use standard identifiers and existing controlled vocabularies

- Data-oriented semantic search of the literature.
- Overcome some of the limitations of keyword-based search

EMBOpress

Data-oriented search

Query:

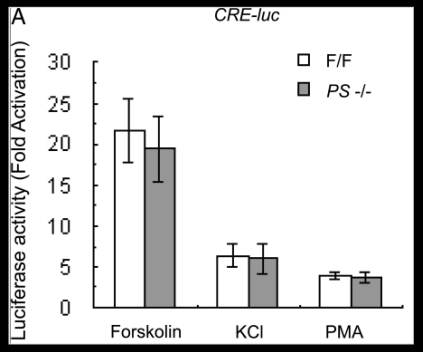

forskolin → CREB

More-like-this:

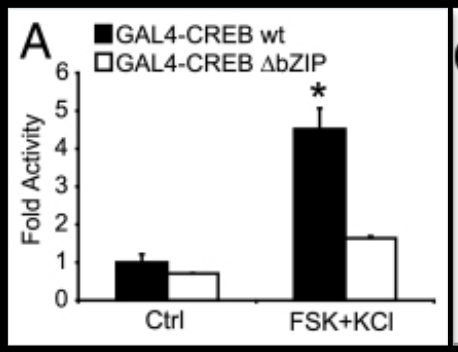

forskolin → CREB

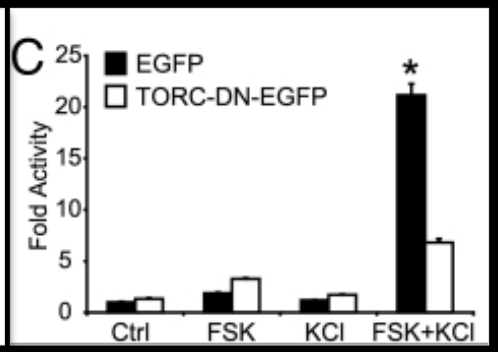

forskolin → CREB

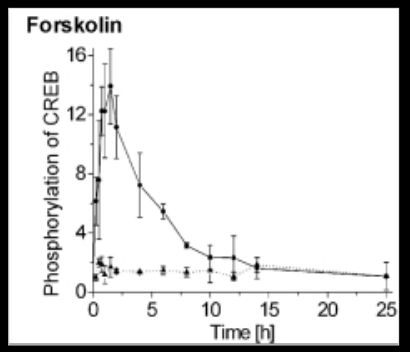

time → CREB

Survey (n=441)
98% of respondents find this function “useful” (42% rate it as “Fantastic!”)

NCBI Resources How To — lemberg My NCBI Sign Out

PubMed.gov — US National Library of Medicine, National Institutes of Health

PubMed | phosphorylated by CDK1 OR CDK1 substrate OR CDK1-dependent phosphorylation OR CD | Search

RSS Save search Advanced — Help

Results: 1 to 20 of 436 << First < Prev Page 1 of 22 Next > Last >>

1. **Cdk1-mediated Phosphorylation** of Receptor Associated Protein 80 (RAP80) Serine 677 Residues Modulate DNA Damage-induced G2/M Checkpoint and Cell Survival.
Cho HJ, Oh YJ, Han SH, Chung HJ, Kim CH, Le NS, m WJ Choi M, Kim H.
J Biol Chem. 2012 Dec 21. [Epub ahead of print]
PMID: 23264621 [PubMed - as supplied by publisher] Fr e Ar cle
Related citations

2. CyclinB1/**Cdk1** phosphorylates mitochondrial antioxidant MnSOD in cell adaptive response to radiation stress.
Candas D, Fan M, Nantajit D, Vaughan AT, Murley J, Woloschak G, Grdina DJ, Li JJ.
J Mol Cell Biol. 2012 Dec 12. [Epub ahead of print]
PMID: 23243068 [PubMed - as supplied by publisher] **Free Article**
Related citations

3. MEK1 inactivates Myt1 to regulate Golgi membrane fragmentation and mitotic entry in mammalian cells.
Villeneuve J, Scarpa M, Ortega-Bellido M, Malhotra V.
EMBO J. 2012 Dec 14. doi: 10.1038/emboj.2012.329. [Epub ahead of print]
PMID: 23241949 [PubMed - as supplied by publisher]
Related citations

4. Sonic hedgehog initiates cochlear hair cell regeneration through downregulation of retinoblastoma protein.
Lu N, Chen Y, Wang Z, Chen G, Lin Q, Chen ZY, Li H.
Biochem Biophys Res Commun. 2012 Dec 2. doi:pii: S0006-291X(12)02278-4. 10.1016/j.bbrc.2012.11.088. [Epub ahead of print]
PMID: 23211596 [PubMed - as supplied by publisher]
Related citations

5. 2-Hydroxyoleic acid induces ER stress and autophagy in various human glioma cell lines.
Marcilla-Etxenike A, Martín ML, Noguera-Salvá MA, García-Verdugo JM, Soriano-Navarro M, Dey I, Escribá PV, Busquets X.
PLoS One. 2012;7(10):e48235. doi: 10.1371/journal.pone.0048235. Epub 2012 Oct 25.
PMID: 23133576 [PubMed - in process] **Free PMC Article**
Related citations

6. Serine **Phosphorylation** Is Critical for the Activation of Ubiquitin-Specific Protease 1 and Its Interaction with WD40-Repeat Protein UAF1.
Villamil MA, Liang Q, Chen J, Choi YS, Hou S, Lee KH, Zhuang Z.
Biochemistry. 2012 Nov 1. [Epub ahead of print]
PMID: 23116119 [PubMed - as supplied by publisher]
Related citations

7. An Unusual Two-Step Control of CPEB Destruction by Pin1.
Nechama M, Lin CL, Richter JD.
Mol Cell Biol. 2013 Jan;33(1):48-58. doi: 10.1128/MCB.00904-12. Epub 2012 Oct 22.
PMID: 23090969 [PubMed - in process]
Related citations

8. Human Cdc14A regulates Wee1 stability by counteracting CDK-mediated **phosphorylation**.
Ovejero S, Ayala P, Bueno A, Sacristán MP.
Mol Biol Cell. 2012 Dec;23(23):4515-25. doi: 10.1091/mbc.E12-04-0260. Epub 2012 Oct 10.
PMID: 23051732 [PubMed - in process]
Related citations

9. **Cdk1** and Plk1 mediate a CLASP2 phospho-switch that stabilizes kinetochore-microtubule attachments.
Maia AR, Garcia Z, Kabeche L, Barisic M, Maffini S, Macedo-Ribeiro S, Cheeseman IM, Compton DA, Kaverina I, Maiato H.
J Cell Biol. 2012 Oct 15;199(2):285-301. doi: 10.1083/jcb.201203091. Epub 2012 Oct 8.

ented search

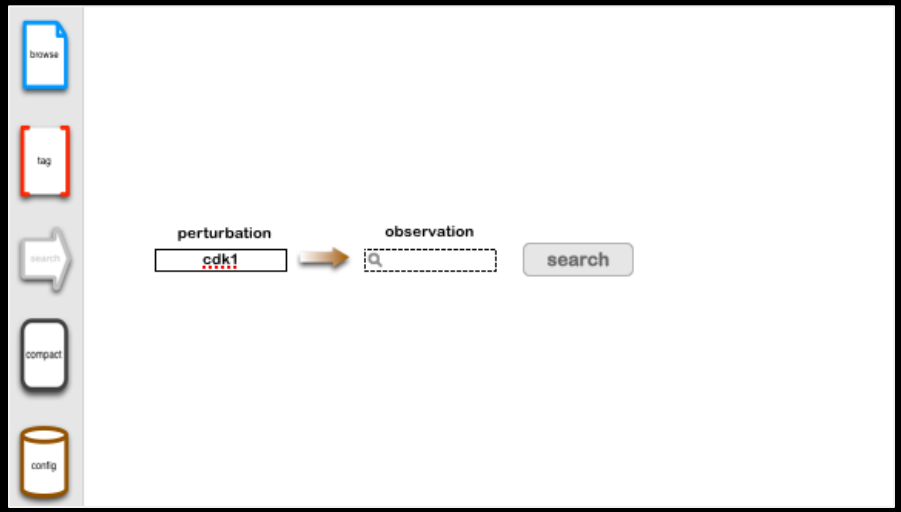

Data-oriented search

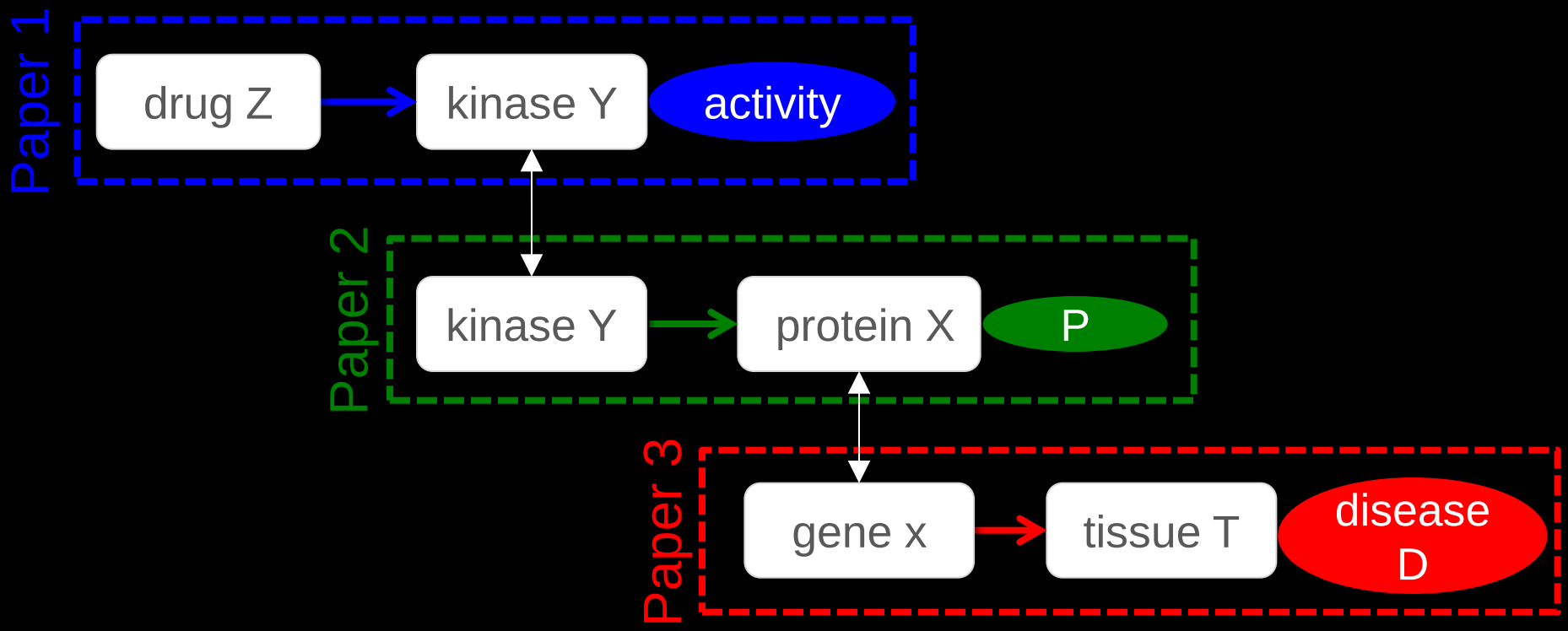

Resulting hypothesis: test drug Z in disease D.

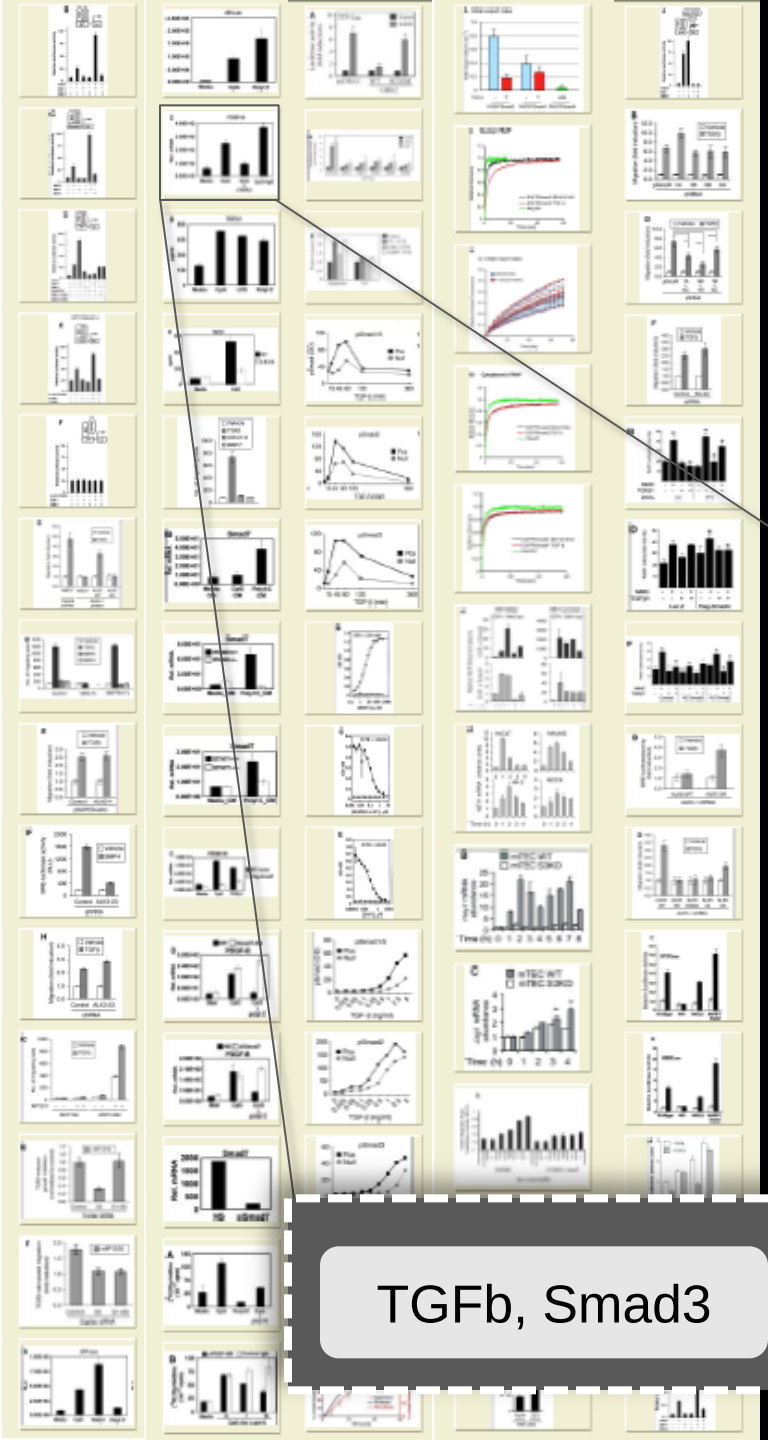

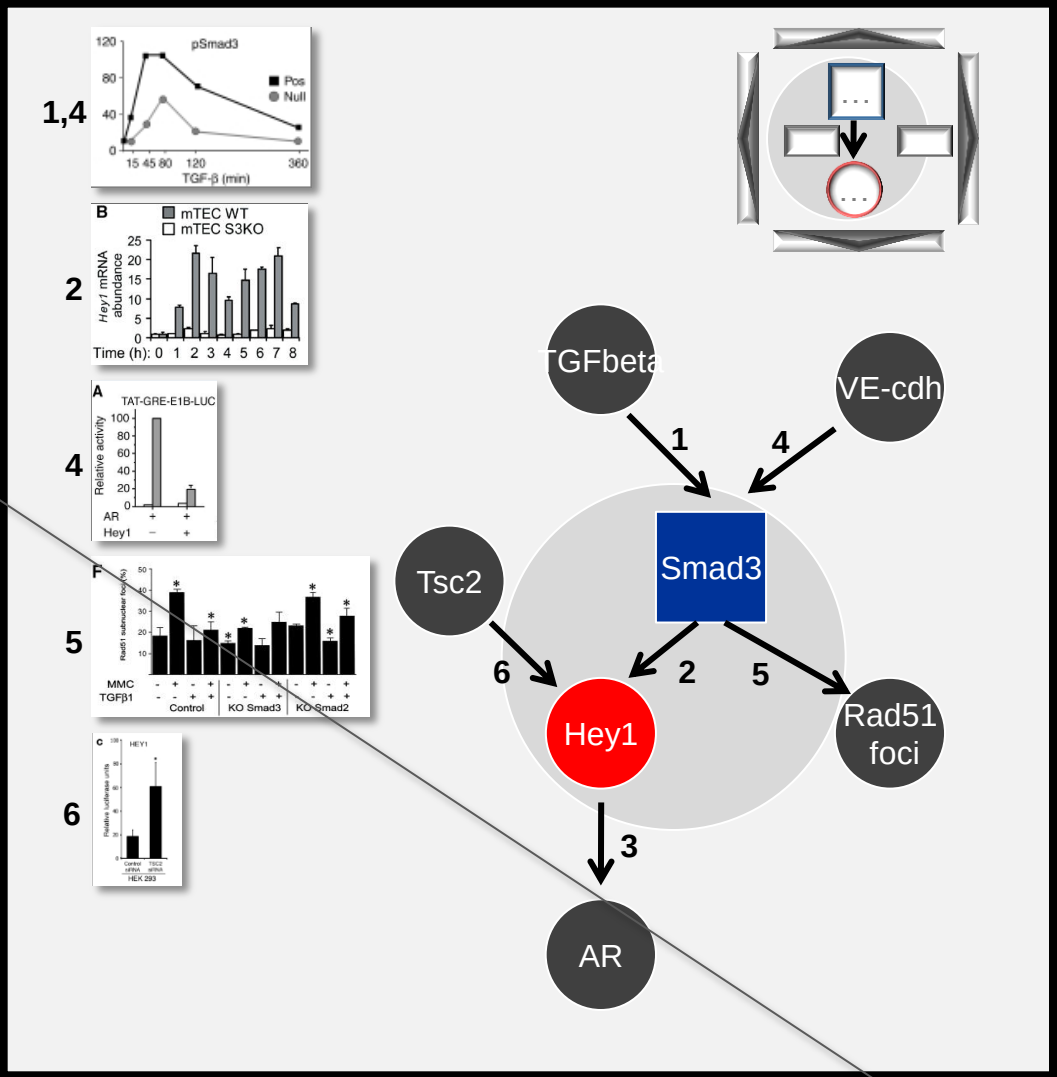

TGFb, Smad3 → Rad51 → Nuclear complexes

Further opportunities

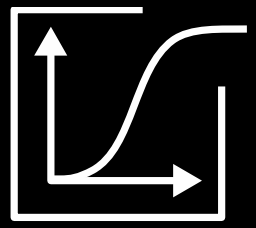

- Context- and network-based ranking metrics
- Linking to external semantic-aware resources
- High level (visual) summarization
- Structured representation of assays
- Use same metadata for data series in datasets

EMBOpress

Publishing as a distributed infrastructure

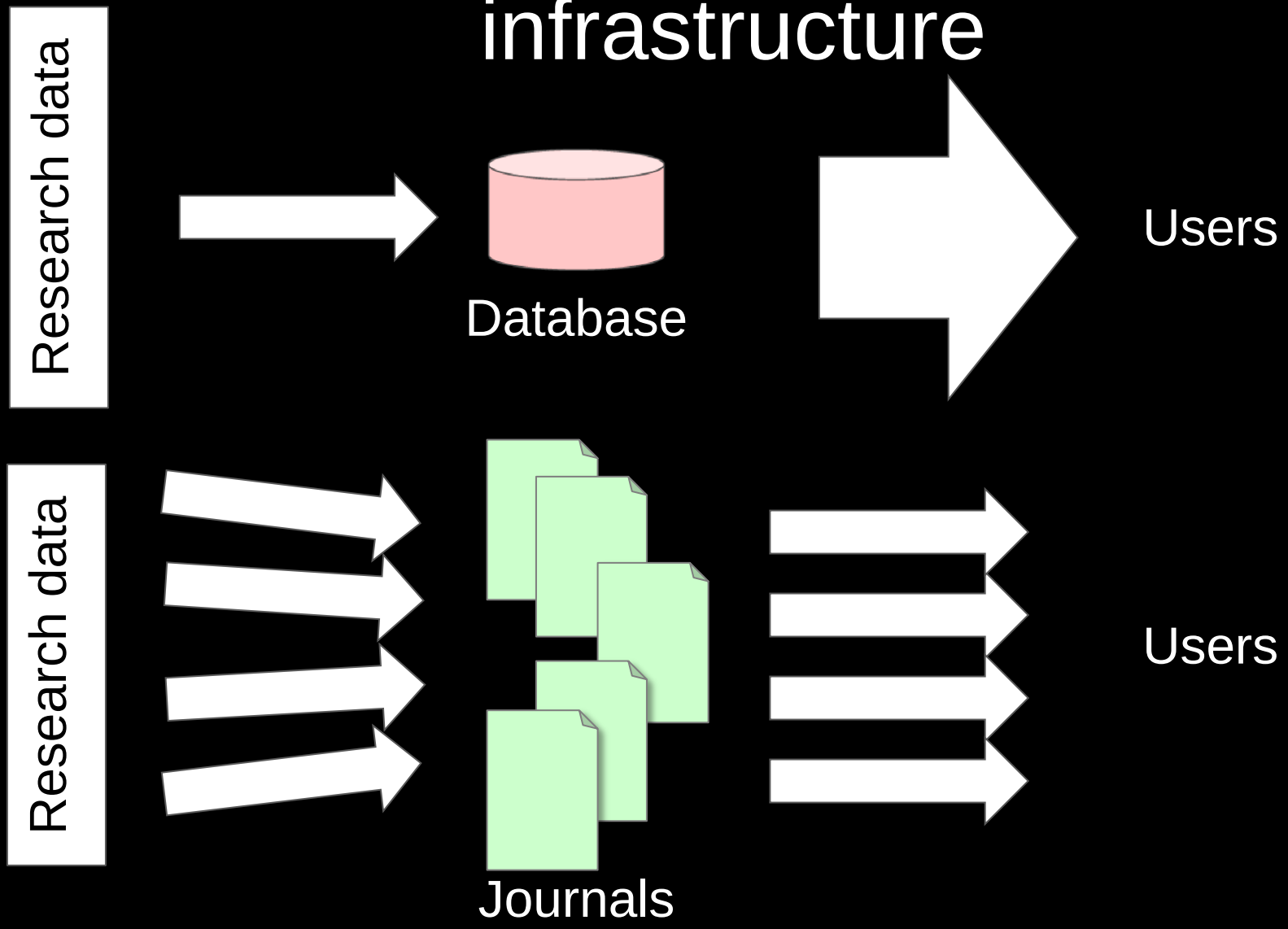

Publishing as a distributed infrastructure

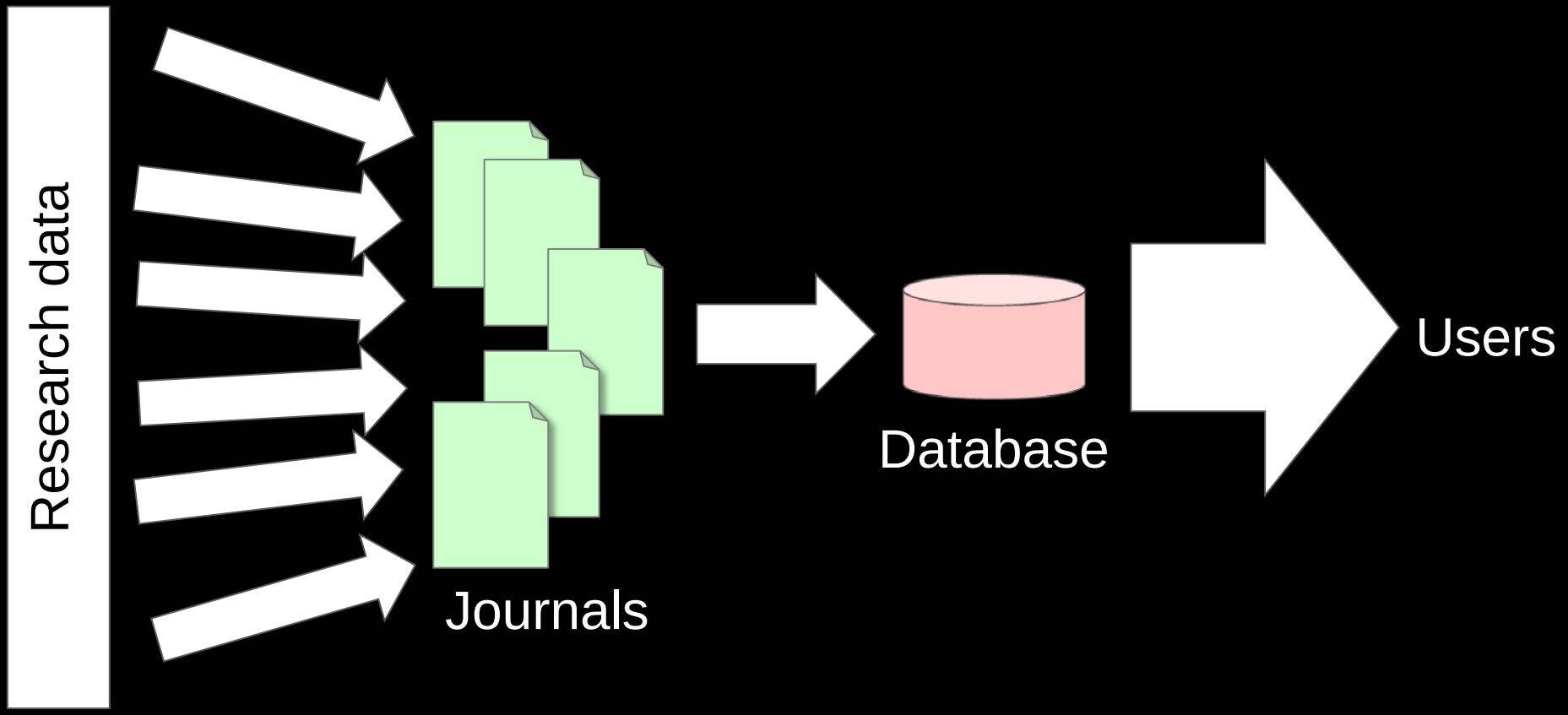

‘Next Gen’ Open Access

EMBOgle

Search | I'm Feeling Lucky | Advanced Search | Language Tools

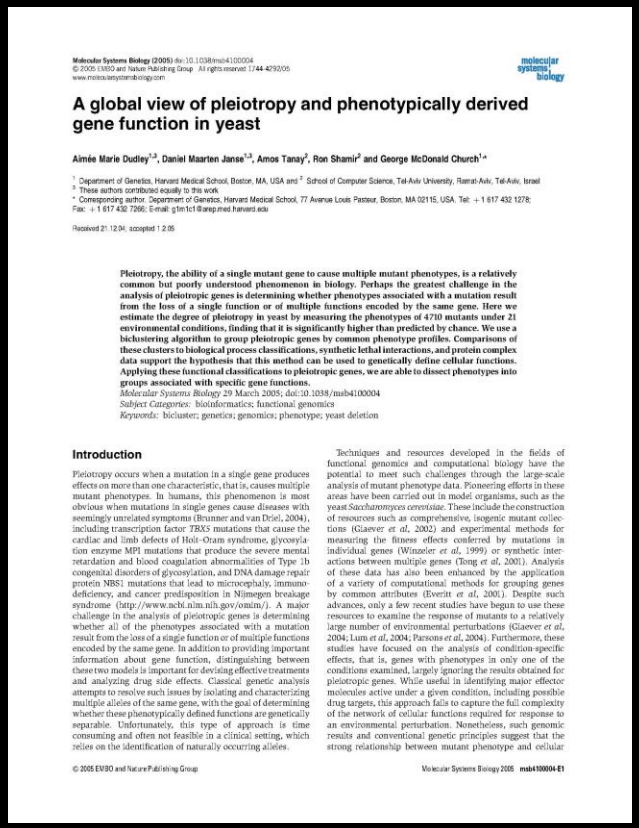

Molecular Systems Biology (2005) doi:10.1038/msb4100004
© 2005 EMBO and Nature Publishing Group All rights reserved 1744-4292/05
www.molecularsystemsbiology.com

molecular systems biology

A global view of pleiotropy and phenotypically derived gene function in yeast

Aimée Marie Dudley[1,2], Daniel Maarten Janse[1,2], Amos Tanay[3], Ron Shamir[3] and George McDonald Church[1,*]

[1] Department of Genetics, Harvard Medical School, Boston, MA, USA and [2] School of Computer Science, Tel-Aviv University, Ramat-Aviv, Tel-Aviv, Israel
[2] These authors contributed equally to this work
* Corresponding author. Department of Genetics, Harvard Medical School, 77 Avenue Louis Pasteur, Boston, MA 02115, USA. Tel: +1 617 432 1278; Fax: +1 617 432 7266; E-mail: gmc1@rascal.med.harvard.edu

Received 21.12.04; accepted 1.2.05

Pleiotropy, the ability of a single mutant gene to cause multiple mutant phenotypes, is a relatively common but poorly understood phenomenon in biology. Perhaps the greatest challenge in the analysis of pleiotropic genes is determining whether phenotypes associated with a mutation result from the loss of a single function or of multiple functions encoded by the same gene. Here we estimate the degree of pleiotropy in yeast by measuring the phenotypes of 4710 mutants under 21 environmental conditions, finding that it is significantly higher than predicted by chance. We use a biclustering algorithm to group pleiotropic genes by common phenotype profiles. Comparisons of these clusters to biological process classifications, synthetic lethal interactions, and protein complex data support the hypothesis that this method can be used to genetically define cellular functions. Applying these functional classifications to pleiotropic genes, we are able to dissect phenotypes into groups associated with specific gene functions.

Molecular Systems Biology 29 March 2005; doi:10.1038/msb4100004
Subject Categories: bioinformatics; functional genomics
Keywords: bicluster; genetics; genomics; phenotype; yeast deletion

Introduction

Pleiotropy occurs when a mutation in a single gene produces effects on more than one characteristic, that is, causes multiple mutant phenotypes. In humans, this phenomenon is most obvious when mutations in single genes cause diseases with seemingly unrelated symptoms (Brunner and van Driel, 2004), including transcription factor *TBX5* mutations that cause the cardiac and limb defects of Holt–Oram syndrome, glycosylation enzyme MPI mutations that produce the severe mental retardation and blood coagulation abnormalities of Type 1b congenital disorders of glycosylation, and DNA damage repair protein NBS1 mutations that lead to microcephaly, immunodeficiency, and cancer predisposition in Nijmegen breakage syndrome (http://www.ncbi.nlm.nih.gov/omim/). A major challenge in the analysis of pleiotropic genes is determining whether all of the phenotypes associated with a mutation result from the loss of a single function or of multiple functions encoded by the same gene. In addition to providing important information about gene function, distinguishing between these two models is important for devising effective treatments and analyzing drug side effects. Classical genetic analysis attempts to resolve such issues by isolating and characterizing multiple alleles of the same gene, with the goal of determining whether these phenotypically defined functions are genetically separable. Unfortunately, this type of approach is time consuming and often not feasible in a clinical setting, which relies on the identification of naturally occurring alleles.

Techniques and resources developed in the fields of functional genomics and computational biology have the potential to meet such challenges through the large-scale analysis of mutant phenotype data. Pioneering efforts in these areas have been carried out in model organisms, such as the yeast *Saccharomyces cerevisiae*. These include the construction of resources such as comprehensive, isogenic mutant collections (Giaever *et al*, 2002) and experimental methods for measuring the fitness effects conferred by mutations in individual genes (Winzeler *et al*, 1999) or synthetic interactions between multiple genes (Tong *et al*, 2001). Analysis of these data has also been enhanced by the application of a variety of computational methods for grouping genes by common attributes (Everitt *et al*, 2001). Despite such advances, only a few recent studies have begun to use these resources to examine the response of mutants to a relatively large number of environmental perturbations (Giaever *et al*, 2004; Lum *et al*, 2004; Parsons *et al*, 2004). Furthermore, these studies have focused on the analysis of condition-specific effects, that is, genes with phenotypes in only one of the conditions examined, largely ignoring the results obtained for pleiotropic genes. While useful in identifying major effector molecules active under a given condition, including possible drug targets, this approach fails to capture the full complexity of the network of cellular functions required for response to an environmental perturbation. Nonetheless, such genomic results and conventional genetic principles suggest that the strong relationship between mutant phenotype and cellular

SOURCE DATA

EMBOpress